DALTON
FULL PAPER

An investigation into the photochemical reactions of M(η^5-C_5H_5)-($CO)_4$ and M(η^5-C_9H_7)($CO)_4$ (M = Nb or Ta) with H_2 and N_2 in polyethylene matrices and liquid xenon at low temperature

Gavin I. Childs,[a] **Skip Gallagher,**[b] **Thomas E. Bitterwolf**[b] **and Michael W. George** *[a]

[a] *School of Chemistry, University of Nottingham, University Park, Nottingham, UK NG7 2RD. E-mail: Mike.George@nottingham.ac.uk*

[b] *Department of Chemistry, University of Idaho, Moscow, ID 83844-2243, USA*

Received 30th August 2000, Accepted 13th October 2000

The photolysis of MCp′$(CO)_4$ (Cp′ = Cp or indenyl; M = Nb or Ta) in polyethylene (PE) matrices at low temperature under a high pressure of reactant gas led to formation of a wide range of photoproducts. Under an inert atmosphere (helium), NbCp′$(CO)_3$ and NbCp′$(CO)_2$ are observed following irradiation of the parent tetracarbonyl. However, only TaCp′$(CO)_3$ is observed for the analogous reactions of the corresponding tantalum compounds. Similarly, NbCp′$(CO)_3(N_2)$ and NbCp′$(CO)_2(N_2)_2$ are seen following irradiation of NbCp′$(CO)_4$ under a high pressure of N_2, whereas only TaCp′$(CO)_3(N_2)$ was observed following irradiation of TaCp′$(CO)_4$. Under hydrogen, the classical dihydride TaCp′$(CO)_3H_2$ is formed following irradiation of TaCp′$(CO)_4$. The non-classical dihydrogen complex Nb(C_9H_7)$(CO)_3$(η^2-H_2) is formed following irradiation of Nb(C_9H_7)$(CO)_4$. NbCp$(CO)_4$ forms both the classical hydride and non-classical dihydrogen complex. Using a high pressure-low temperature cell, the thermal reaction of TaCp′$(CO)_3(N_2)$ with hydrogen to form TaCp′$(CO)_3H_2$ was observed. Preliminary room temperature studies suggest that Ta(C_9H_7)$(CO)_3H_2$ is *ca.* 50 times more reactive than TaCp$(CO)_3H_2$ in PE.

Introduction

Transition metal dihydride and dihydrogen complexes are of fundamental interest due to the important role these complexes play as intermediates in a number of catalytic hydrogenation processes.[1–3] Transition metal dihydrides have a long history whereas the first isolable dihydrogen complex was only reported by Kubas *et al.*[4] in 1984. The coordination of dinitrogen to transition metals is of interest because of its relevance to nitrogen fixation.[5,6] A variety of spectroscopic techniques have played an important role in the understanding of unstable organometallic dihydrogen, dihydride and dinitrogen complexes. A wide range of dinitrogen complexes have been generated by photolysis of metal carbonyl complexes in nitrogen matrices at cryogenic temperatures.[7,8] Similarly, low temperature matrix isolation[9–13] has also been used to characterise non-classical dihydrogen complexes including M$(CO)_5$(η^2-H_2) (M = Cr, Mo or W), Cr$(CO)_4$(η^2-H_2)$_2$, *cis*- and *trans*-MCp-$(CO)_2$(η^2-H_2) (M = Mo or W) and Pd(η^2-H_2). Matrix isolation is a powerful technique for characterising unstable complexes. However, this method gives limited information concerning the stability and reactivity of unstable intermediates.

Dinitrogen and non-classical dihydrogen complexes can also be generated by photolysis of an appropriate metal carbonyl dissolved in liquefied xenon (lXe) doped with nitrogen or hydrogen at cryogenic temperatures.[14–17] The complete miscibility of both hydrogen and nitrogen with supercritical fluids has enabled the characterisation of a variety of unstable dihydrogen and dinitrogen complexes in supercritical xenon doped with a high pressure of reactant gas at ambient temperature using conventional IR spectroscopy.[18,19] This approach has allowed the characterisation[18] and then the isolation[20] of MnCp$(CO)_2$-(η^2-H_2). Time-resolved infrared spectroscopy (TRIR), a combination of flash photolysis and infrared detection, has been a useful technique to probe the formation and reactivity of unstable organometallic dihydrogen and dinitrogen complexes at room temperature in solution.[21–23]

There have been relatively few investigations concerning the photochemistry of the Group 5 carbonyl compounds. V(η^5-C_5R_5)$(CO)_3(N_2)$ (R = H, Me, or Cl), V(η^5-C_5H_4Me)$(CO)_3(N_2)$, V(η^5-C_9H_7)$(CO)_3(N_2)$ and V(η^5-C_5Me_5)$(CO)_2(N_2)_2$ have been observed[24,25] following irradiation of the parent tetracarbonyl complexes in frozen nitrogen matrices at 12 K. The unsaturated complexes V(η^5-C_5R_5)$(CO)_x$ (R = H, Me, or Cl; $x = 2$ or 3), V(η^5-C_5H_4Me)$(CO)_x$ ($x = 2$ or 3) and V(η^5-C_9H_7)$(CO)_3$ were observed following irradiation in frozen inert matrices. Photolysis of MCp′$(CO)_4$ (M = Nb or Ta; Cp′ = Cp or indenyl) in frozen Nujol[26] yielded the unsaturated CO-loss products MCp′$(CO)_3$ and MCp′$(CO)_2$. Irradiation of V(η^5-C_5R_5)$(CO)_4$, V(η^5-C_9H_7)$(CO)_4$, V(η^5-C_5Me_5)$(CO)_4$ and MCp′$(CO)_4$ (M = Nb or Ta) also yielded additional photoproducts which were tentatively assigned to the ring-slip products V(η^3-C_5R_5)$(CO)_4$, V(η^3-C_9H_7)$(CO)_4$, V(η^3-C_5Me_5)$(CO)_4$ and M(η^3-Cp′)$(CO)_4$, where the hapticity of the cyclopentadienyl or indenyl ring has shifted from 5 to 3. However, recent[27] ultrafast infrared studies on VCp$(CO)_4$ have suggested an alternative assignment, with an additional band (at 2020 cm^{-1}) observed upon photolysis being attributed to the triplet state of VCp$(CO)_3$.

The combination of liquid xenon at cryogenic temperatures and fast TRIR at room temperature has been used to probe the photochemistry of the Group 5 complexes MCp$(CO)_4$ (M = V, Nb or Ta) in the presence of both dinitrogen and dihydrogen.[28–30] Formation of MCp$(CO)_{4-n}(N_2)_n$ ($n = 1$ or 2 (Nb only)) was observed for the reactions in the presence of dinitrogen. However, the reactions under dihydrogen gave contrasting results. For V the non-classical dihydrogen complex VCp$(CO)_3$-(H_2) was formed, whereas for Ta the classical dihydride complex TaCp$(CO)_3H_2$ was formed. For Nb both the non-classical NbCp$(CO)_3$(η^2-H_2) and the classical NbCp$(CO)_3H_2$ complexes were observed. Furthermore, these complexes were found to be in rapid equilibrium. It was also observed that VCp$(CO)_3$-(η^2-H_2) reacts thermally with N_2 in liquid xenon to form VCp$(CO)_3(N_2)$.

DOI: 10.1039/b007023h

A new matrix isolation technique involving high pressures and low temperatures, designed to complement conventional low temperature techniques, has been reported.[31] This technique was an extension of Rest's work on polymer matrices,[32] and employs a miniature high-pressure cell attached to a matrix isolation apparatus. The organometallic starting material is impregnated into polymer and surrounded by a high pressure of gas. Irradiation of the cooled matrix allows the generation of unstable organometallic compounds. The thermal reactions of the unstable organometallic compound can then be monitored. This approach has been used to generate $Fe(CO)_4N_2$ in polyethylene (PE) at 190 K and follow its thermal reaction with H_2.[31] It has also been used to generate $M(\eta^6\text{-}C_6H_3Me_3\text{-}1,3,5)(CO)_{3-n}(N_2)_n$ (n = 1–3), $M(\eta^6\text{-}C_6H_3Me_3\text{-}1,3,5)(CO)_2(H_2)$ (M = Cr or Mo), *cis*-$W(CO)_4(H_2)(CS)$ and *trans*-$W(CO)_4(H_2)(CS)$ and monitor their reaction chemistry.[33]

In this paper we investigate the photochemical reactions of $MCp'(CO)_4$ **1**–**4** (Cp′ = Cp or Indenyl; M = Nb or Ta) with H_2 and N_2 in polyethylene matrices at low temperature. We have utilised the advantages of using polymer matrices to study the thermal reactions of the photoproducts formed at low temperature.

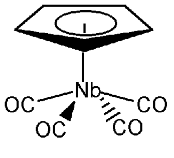

1

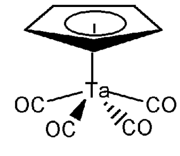

2

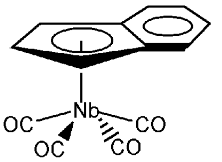

3

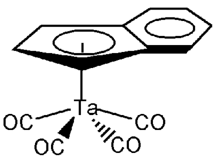

4

Results and discussion

Photolysis of compounds 1–4 in PE matrices in the absence of reactant gas

The infrared spectra of compounds **1**–**4** in PE all have three ν(C–O) bands compared to two ν(C–O) bands observed when **1**–**4** are dissolved in solution (*e.g.* *n*-heptane). The extra band can be attributed to the IR-inactive b_1 stretch, indicating some deviation from strict C_{4v} local symmetry when these compounds are dissolved in the polymer. Photolysis of **1** at 100 K under an inert atmosphere (500 psi of helium) results in a decrease in intensity of the three parent bands, concurrent with production of a new photoproduct with three ν(C–O) bands (see Fig. 1). This photoproduct can be assigned to the unsaturated CO-loss product, $NbCp(CO)_3$ **1A**, by comparison to results from matrix isolation experiments and room temperature TRIR measurements[26,30] (see Table 1). The presence of an additional IR band at 2131 cm^{-1} due to 'free' CO aids this assignment. Similarly, irradiation of **2**, **3** and **4** in PE at 100 K results in the formation of the unsaturated intermediates $TaCp(CO)_3$ **2A**, $Nb(C_9H_7)(CO)_3$ **3A** and $Ta(C_9H_7)(CO)_3$ **4A** (Fig. 1). Further photolysis of **1** and **3** leads to the growth of a new secondary photoproduct with two ν(C–O) bands. These two new bands appear at wavenumbers lower than those for **1A** and **3A**, and can be assigned to the double-CO loss products $NbCp(CO)_2$ **1A′** and $Nb(C_9H_7)(CO)_2$ **3A′**. **1A′** and **3A′** could be either *cis* or *trans*, but by analogy to previous results obtained in frozen Nujol[26] it is likely that the bands observed are due to the *cis* isomer.[34] No evidence for formation of the *trans* isomer was seen, and production of tricarbonyl-loss fragments was also not observed. Further photolysis of **2** and **4** produced no evidence for formation of double-CO loss products. Previous studies in frozen Nujol[26] and frozen gas matrices[24,25] have observed photoproducts which have been assigned to ring-slip species. However, in all of the experiments performed in this investigation no evidence for photoproducts with IR bands previously[24–26] assigned to ring-slip species were observed. Upon warming the polymer disc to 150 K, all of the new photoproducts decay away to reform the parent compounds, **1**–**4**. The band positions of the photoproducts generated in these experiments are shown in Table 1.

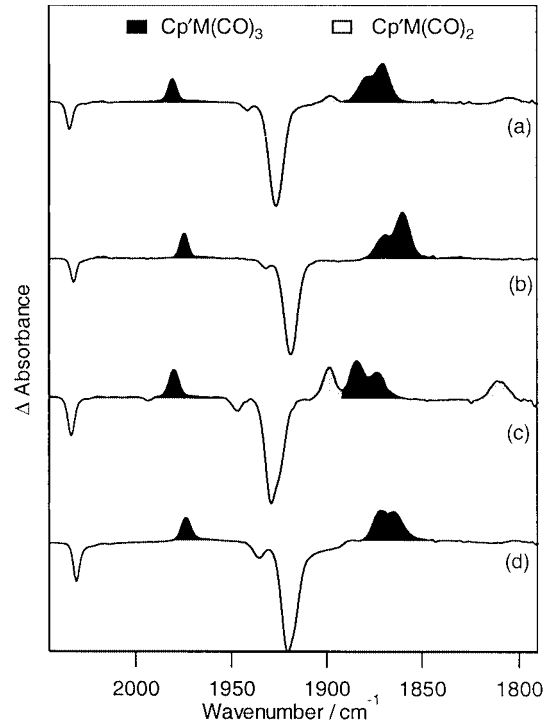

Fig. 1 FTIR difference spectra following UV irradiation of $MCp'(CO)_4$ at 100 K under helium in PE discs (a = **1**, b = **2**, c = **3**, d = **4**). Negative peaks are due to depletion of parent, with positive peaks due to formation of new species.

All of the experiments described above were repeated under a pressure of CO (900 psi) to try and observe the formation of ring-slip species. However, upon photolysis identical results were obtained to those observed under a high pressure of helium.

Photolysis of compounds 1–4 in PE matrices in the presence of nitrogen

Fig. 2 shows the IR spectra obtained following irradiation of compounds **1**–**4** under N_2 (900 psi) at 160 K. Upon photolysis the parent ν(C–O) bands decrease in intensity and new photoproducts are formed with three ν(C–O) bands and one ν(NN) stretch at *ca.* 2200 cm^{-1} (see Table 2). These results suggest substitution of one CO group for a N_2 ligand, forming $NbCp(CO)_3(N_2)$ **1B**, $TaCp(CO)_3(N_2)$ **2B**, $Nb(C_9H_7)(CO)_3(N_2)$ **3B** and $Ta(C_9H_7)(CO)_3(N_2)$ **4B**. Upon further irradiation of **1** and **3**, a secondary photoproduct with a single carbonyl stretch and two new ν(NN) stretches was observed (Table 2). The presence of two dinitrogen stretches, well separated in frequency, indicates the presence of two dinitrogen groups coordinated to the metal centre. These secondary photoproducts can be assigned to the disubstituted species $NbCp(CO)_2(N_2)_2$ **1B′** and $Nb(C_9H_7)(CO)_2(N_2)_2$ **3B′**. The relative intensities of the dinitrogen stretches[34] indicate that these secondary photoproducts are the *cis* isomeric form. The *cis* isomer would be expected to have two ν(C–O) stretches, whereas only one has been observed. However, the second band may well be obscured by the ν(C–O) stretches of either the parent tetracarbonyls or the monosubstituted primary photoproducts. These observations are consistent with the results previously obtained[30] in liquid xenon studies. Further photolysis of **2** and **4** did not yield any addi-

Table 1 IR band positions (cm^{-1}) of MCp′(CO)$_{4-x}$ (Cp′ = Cp or indenyl; M = Nb or Ta; x = 0, 1 or 2) species. For the unsaturated compounds the vacant site is filled by coordination to the matrix material

Compound	PE (100 K)[a]	lXe (203 K)[b]	*n*-Heptane (298 K)[b]	Nujol matrix (77 K)[c]	Frozen gas matrix (12 K)[b]
1 NbCp(CO)$_4$	2035	2038.5	2037	2034	
	1942.5	1933.5	1932	1942	
	1927			1927	
1A NbCp(CO)$_3$	1980.5		1986	1982	
	1877.5		1885[d]	1881	
	1870			1871	
1A′ *cis*-NbCp(CO)$_2$	1898			1898	
	1804			1804	
trans-NbCp(CO)$_2$	not seen			2006	
2 TaCp(CO)$_4$	2032.5	2036	2033.5	2033	2038
	1932	1925.5	1923	1934	1930.5
	1919			1918	
2A TaCp(CO)$_3$	1974		1980	1977	1987
	1868		1880	1872	1880
	1860		1873	1859	1874
3 Nb(C$_9$H$_7$)(CO)$_4$	2034			2034	
	1947			1947	
	1929.5			1930	
3A Nb(C$_9$H$_7$)(CO)$_3$	1980			1980	
	1884			1883	
	1873.5			1873	
3A′ *cis*-Nb(C$_9$H$_7$)(CO)$_2$	1899			1899	
	1810			1809	
trans-Nb(C$_9$H$_7$)(CO)$_2$	not seen			1991	
				1905	
4 Ta(C$_9$H$_7$)(CO)$_4$	2031			2032	
	1935.5			1937	
	1921			1921	
4A Ta(C$_9$H$_7$)(CO)$_3$	1973.5			1975	
	1871.5			1873	
	1865			1864	

[a] This study. [b] See reference 30. [c] See reference 26. [d] Unresolved peaks.

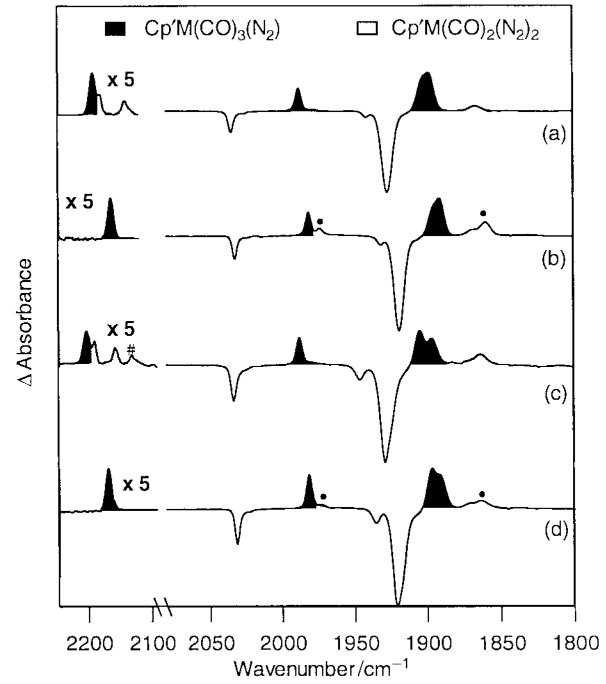

Fig. 2 FTIR difference spectra following UV irradiation of MCp′(CO)$_4$ at 160 K under nitrogen in PE discs (a = **1**, b = **2**, c = **3**, d = **4**). Negative peaks are due to depletion of parent, with positive peaks due to formation of new species. Peaks marked ● are due to formation of the CO-loss tricarbonyl species (**2A** or **4A**), and the peak marked # is due to 'free' CO.

tional photoproducts. Moreover, in all of our investigations under N$_2$, there was no evidence for generation of photoproducts with ν(C–O) bands previously[25] assigned to ring-slip species. The photoproducts **1B**, **1B′**, **2B**, **3B**, **3B′**, and **4B** are thermally stable in the PE discs at 160 K. Warming the PE discs to 260 K resulted in decay of the bands due to the dinitrogen bound species along with regeneration of the parent bands. The band positions of all the photoproducts are collected in Table 1.

These results obtained under a reactive gas (N$_2$) are consistent with those observed under an inert gas (He). Disubstitution was observed for both of the niobium compounds and monosubstitution for the tantalum compounds. Why the NbCp′(CO)$_4$ complexes apparently undergo polysubstitution more easily than the TaCp′(CO)$_4$ remains unclear.

Photolysis of compounds 1–4 in PE matrices and liquid xenon in the presence of hydrogen

Fig. 3 shows the IR spectra obtained following UV photolysis of compounds **1**–**4** in PE under hydrogen (900 psi) at 170 K. Upon irradiation of **2** and **4** a decrease in the parent bands is observed, concurrent with a growth in three new carbonyl stretches *higher* in frequency than the parent bands (Table 3).[35] This indicates oxidation of the metal centre from Ta^{I} to Ta^{III}, following oxidative addition of H$_2$ to Ta to form the classical dihydride species TaCp(CO)$_3$H$_2$ **2C** and Ta(C$_9$H$_7$)(CO)$_3$H$_2$ **4C**. No metal–hydride ν(M–H) IR bands were observed. Formation of a dihydride by third row elements is consistent with results seen for Group 7 and 8 compounds.[18,36] Third row complexes have increased back bonding from the metal centre to the coordinated dihydrogen. This results in overpopulation of the unoccupied σ* orbital of the dihydrogen, causing cleavage of the H–H bond to form the classical dihydride. The increase in coordination number upon formation of a dihydride complex also means that this type of complex is favoured for the third-row transition metal complexes. Both **2C** and **4C** were thermally stable in the PE discs at 170 K, and decayed gradually as the PE disc was warmed to room temperature.

Table 2 IR band positions (cm^{-1}) of $MCp'(CO)_{4-x}(N_2)_x$ (Cp′ = Cp or indenyl; M = Nb or Ta; x = 1 or 2) species

Compound	PE (160 K)[a]	lXe (203 K)[b]	*n*-Heptane (298 K)[b]	Frozen gas matrix (12 K)[b]
1B $NbCp(CO)_3(N_2)$	2191	2193	[c]	
	1988	1992.5	1993	
	1898.5[d]	1906[d]	1903[d]	
1B′ *cis*-$NbCp(CO)_2(N_2)_2$	2179.5	2180		
	2140.5	2141		
	1865.5	1873		
2B $TaCp(CO)_3(N_2)$	2163	2164	[c]	[c]
	1981.5	1986	1987	1906
	1891.5[d]	1899[d]	1903[d]	1900
3B $Nb(C_9H_7)(CO)_3(N_2)$	2202			
	1988			
	1905			
	1897			
3B′ *cis*-$Nb(C_9H_7)(CO)_2(N_2)_2$	2190			
	2157			
	1864			
4B $Ta(C_9H_7)(CO)_3(N_2)$	2172.5			
	1981.5			
	1897			
	1892			

[a] This study. [b] See reference 32. [c] Expected band not observed. [d] Unresolved peaks.

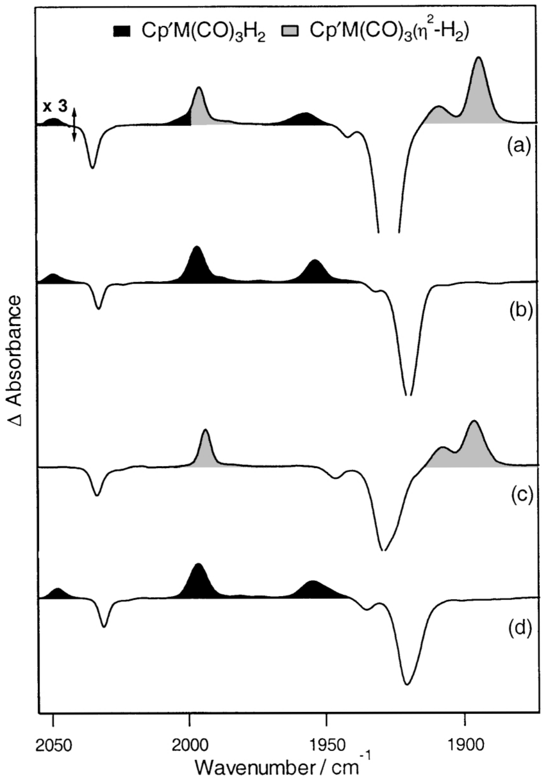

Fig. 3 FTIR difference spectra following UV irradiation of $MCp'(CO)_4$ at 170 K under hydrogen in PE discs (a = **1**, b = **2**, c = **3**, d = **4**). Negative peaks are due to depletion of parent, with positive peaks due to formation of new species. In (a) the region 2045–2055 cm^{-1} has been enhanced for ease of viewing.

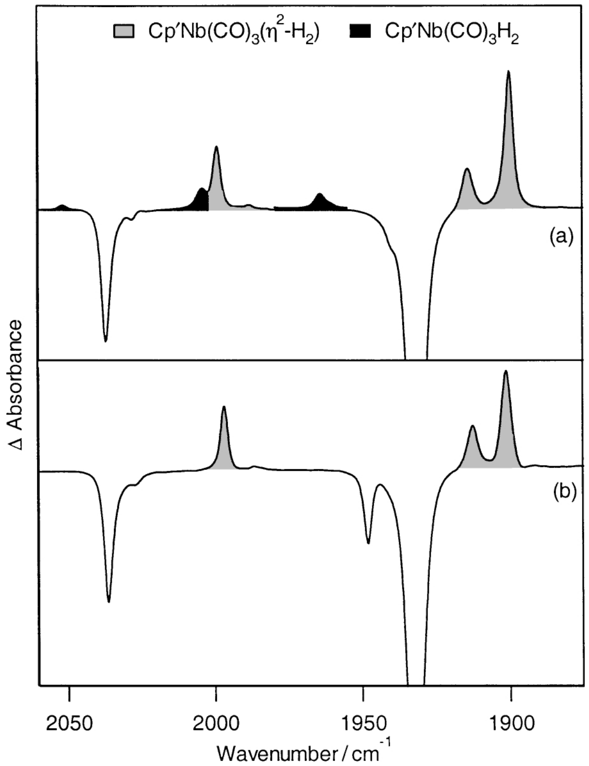

Fig. 4 FTIR difference spectra following UV irradiation of $NbCp'(CO)_4$ in lXe doped with hydrogen at 170 K (a = **1**, b = **3**). Negative peaks are due to depletion of parent, with positive peaks due to formation of new species.

Upon photolysis of compound **1** six new bands are observed (Fig. 3, Table 3). By analogy with previous[29,30] studies it is clear that these are due to formation of both the classical dihydride, $NbCp(CO)_3H_2$ **1C**, and the non-classical dihydrogen complex, $NbCp(CO)_3(\eta^2\text{-}H_2)$ **1D**. However, upon irradiation of **3**, the indenyl analogue of **1**, only three new bands are observed at wavenumbers *lower* than those of the parent.[35] These are in positions similar to those of the dinitrogen complex **3B**, and can be assigned to the non-classical dihydrogen complex $Nb(C_9H_7)(CO)_3(\eta^2\text{-}H_2)$ **3D**. The formation of **1C** and **1D** has previously been observed in liquid xenon. In order to probe whether the observation of only the dihydrogen complex, **3D**, in PE was in part due to the PE matrix, we have repeated the irradiation of **1** and **3** in liquid xenon doped with hydrogen (see Fig. 4). Identical results to those obtained in the PE experiments were observed, with formation of both the dihydride (**1C**) and dihydrogen (**1D**) complexes seen following photolysis of **1**, and formation of only the dihydrogen complex (**3D**) seen following irradiation of **3**. We found no evidence for formation of the classical dihydride, $Nb(C_9H_7)(CO)_3H_2$ **3C**. The reason why photolysis of $NbCp(CO)_4$ results in the formation of both classical and non-classical dihydrogen complexes, whereas only a non-classical dihydrogen complex is detected following irradiation of $Nb(C_9H_7)(CO)_4$ in the presence of H_2, may be due to only a

Table 3 IR band positions (cm^{-1}) of $MCp(CO)_3(X_2)$ (Cp′ = Cp or indenyl; M = Nb or Ta; X = H_2 or η^2-H_2) species

Compound	PE (160 K)[a]	lXe (203 K)	*n*-Heptane (298 K)[b]
1D $NbCp(CO)_3(\eta^2\text{-}H_2)$	1995.5	2001[a,b]	[c]
	1908	1915[a,b]	1912
	1894	1902[a,b]	1904
1C $NbCp(CO)_3H_2$	2049	2053[a,b]	[c]
	2001	2006[a,b]	[c]
	1956.5	1966[a,b]	1969
2C $TaCp(CO)_3H_2$	2049	2053.5[b]	[c]
	1996	2002[b]	[c]
	1959	1958.5[b]	1960[d]
3D $Nb(C_9H_7)(CO)_3(\eta^2\text{-}H_2)$	1993.5	1997[a]	
	1907.5	1912.5[a]	
	1896	1901[a]	
4C $Ta(C_9H_7)(CO)_3H_2$	2048		
	1996.5		
	1954.5		

[a] This study. [b] See reference 30. [c] Expected band not observed. [d] Unresolved peaks.

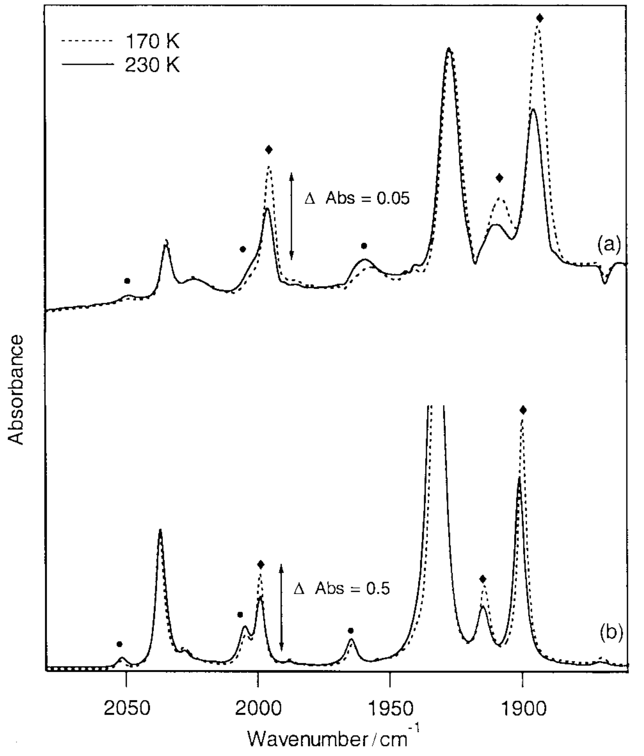

Fig. 5 FTIR obtained following warming of a (a) PE disc and (b) lXe containing $NbCp(CO)_4$ (**1**) from 170 to 230 K. Upon warming the peaks due to **1C** (marked ●) increase in intensity and the peaks due to **1D** (marked ◆) decrease in intensity.

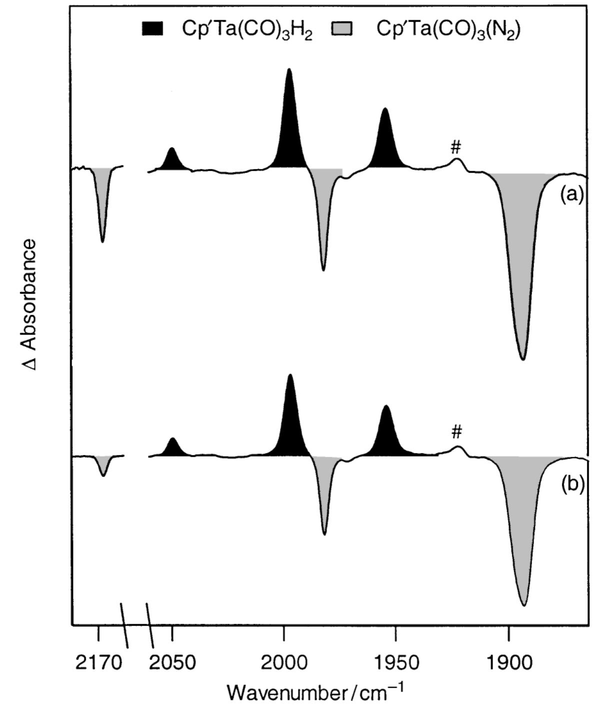

Fig. 6 FTIR difference spectra obtained following warming of a PE disc containing (a) **2B** and (b) **4B** from 160 to 280 K under hydrogen (900 psi). Negative peaks are due to depletion of nitrogen-bound species, with positive peaks due to formation of new hydrogen-bound species. Peaks marked # are due to incomplete parent subtraction.

small change in the relative energies of these complexes. The fact that both **1C** and **1D** are formed means that there is only a small energy difference between these complexes. Indeed, in our earlier liquid xenon studies[30] we determined that **1C** is only marginally higher in energy than **1D**.

Previous lXe experiments have shown that compounds **1C** and **1D** are in rapid equilibrium. Warming the reaction mixture from 170 K to 230 K led to conversion of **1D** into **1C**, a process that was reversed upon recooling the mixture. Upon warming the PE disc containing **1C** and **1D** an identical process was observed, with an increase in the bands due to **1C** at the expense of the bands due to **1D** (see Fig. 5). However, upon cooling the polymer disc the reverse process was not observed, with the peaks due to both **1C** and **1D** thermally decaying, and parent peaks (**1**) being regenerated. In the PE experiments, cooling the PE disc from 230 to 170 K takes much longer than cooling liquid xenon over the same temperature range. This means that **1C** and **1D** are kept at the higher temperature for longer periods of time when in the PE matrix, increasing the likelihood of thermal decay back to parent. Warming both the PE disc and the lXe solution containing **3D** produced no evidence for formation of **3C**, with the bands due to **3D** thermally decaying at around 230 K in both cases.

Thermal reaction of compounds 2B and 4B with hydrogen in PE discs

The use of polymer matrices has many advantages compared to more conventional matrix materials. One of the major benefits is the ease with which gases can be vented and added to the polymer, enabling gas exchange reactions to be monitored. If a polymer disc containing the dinitrogen complex **2B**, formed by photolysis of **2** under nitrogen, is warmed from 160 to 280 K under a pressure of hydrogen (900 psi) a decrease in the carbonyl stretches attributable to **2B** is observed. As the bands due to **2B** decay away, there is a concurrent growth in three new bands at higher wavenumbers that can be assigned to the

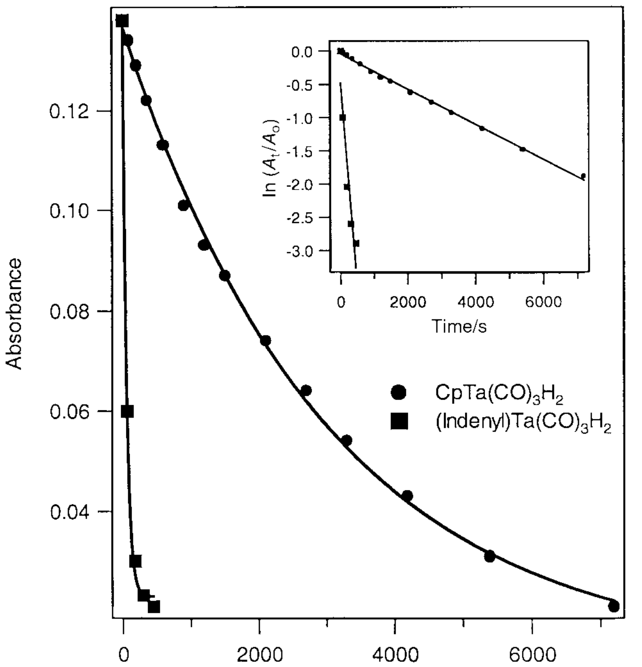

Fig. 7 Plots of absorbance against time showing the decay rates of both $TaCp(CO)_3H_2$ and $Ta(C_9H_7)(CO)_3H_2$. The plots have been fitted to first order kinetics and autoscaled for ease of viewing. The inset shows plots of ln (A_t/A_0) against time, where A_t is absorbance after time, t, and A_0 the original absorbance.

dihydride complex **2C** (see Fig. 6). Analogous results are obtained when **4B** is warmed under a pressure of hydrogen, with **4C** being formed (Fig. 6). These results suggest that the dihydride species **2C** and **4C** are thermally more stable than the corresponding dinitrogen complexes, **2B** and **4B**. This result contrasts with a range of non-classical dihydrogen complexes,[14,15] where the corresponding dinitrogen species are more stable, and the dihydrogen group can easily be displaced by N_2. Unfortunately we have been unable to observe thermal conversion of the dihydrogen complexes **1D** and **3D** to the dinitrogen complexes **1B** and **3B** in this study, with reformation of the parents **1** and **3** seen when **1D** and **3D** are warmed under nitrogen. This may be because gases are inefficiently[33] vented at low temperature (<210 K). We have previously demonstrated[33] that effective venting of H_2 only occurs above 220 K, and N_2 only enters PE efficiently at temperatures above 220 K. This means photodissociated CO may be trapped in the polymer and unable to diffuse away from the dihydrogen bound species. Upon warming the PE disc, **1D** and **3D** can recombine with the CO to reform the parent complexes rather than reacting with N_2 to form **1B** and **3B**. In the successful thermal exchange reactions described above this is not the case, because the dihydride complexes (**2C** and **4C**) are stable at higher temperatures meaning gases can be vented efficiently and photodissociated CO does not become trapped.

Decay of compounds 2C and 4C in PE discs under hydrogen at room temperature

As seen previously, both compounds **2C** and **4C** can be observed in PE discs up to 298 K, and this gives us the opportunity to compare the lifetimes of these species at room temperature. Both **2C** and **4C** were generated (see above), and the absorbance of these species was monitored as a function of time. From Fig. 7 it is clear that **4C** (lifetime *ca.* 1 min) is far more reactive than **2C** (lifetime *ca.* 50 min). As **2C** and **4C** decay, no evidence for regrowth of parent is seen. Additionally, no new IR bands are observed. This is either due to the formation of a product with no strong IR absorptions, or to precipitation of product in the PE disc.

The reaction of PPh_3 with $RhCp(CO)_2$ is 8 orders of magnitude slower than the analogous reaction with $Rh(C_9H_7)(CO)_2$.[37] This suggests that a ring-slip intermediate plays a major role in the increased reactivity of the indenyl complex. Recent time resolved studies[38] by Ford and co-workers have found that the photodecarbonylation of $Fe(C_9H_7)(CO)_2(C(O)CH_3)$ at room temperature is *ca.* 5 times faster than photodecarbonylation of $FeCp(CO)_2(C(O)CH_3)$. No ring-slip products were observed in this study, and the authors suggest that the five-fold difference in reactivity was not great enough to support a ring-slip mechanism. The difference in reactivity of **2C** and **4C** observed in this study is relatively small. Although the increased reactivity of **4C** compared to **2C** is *ca.* 10 times greater than the difference in reactivity between $Fe(C_9H_7)(CO)_2(C(O)CH_3)$ and $FeCp(CO)_2(C(O)CH_3)$, it is much smaller than the difference in reactivity of $Rh(C_9H_7)(CO)_2$ and $RhCp(CO)_2$ towards PPh_3. Thus although there is an effect on the decay of the dihydride complexes, any contribution from decay *via* a ring-slipped intermediate is not as large as previously observed in other systems. Unfortunately the other hydrogen and nitrogen bound complexes characterised in this study are too short-lived to have their kinetics measured using conventional FTIR, and we are currently investigating the reactivities of

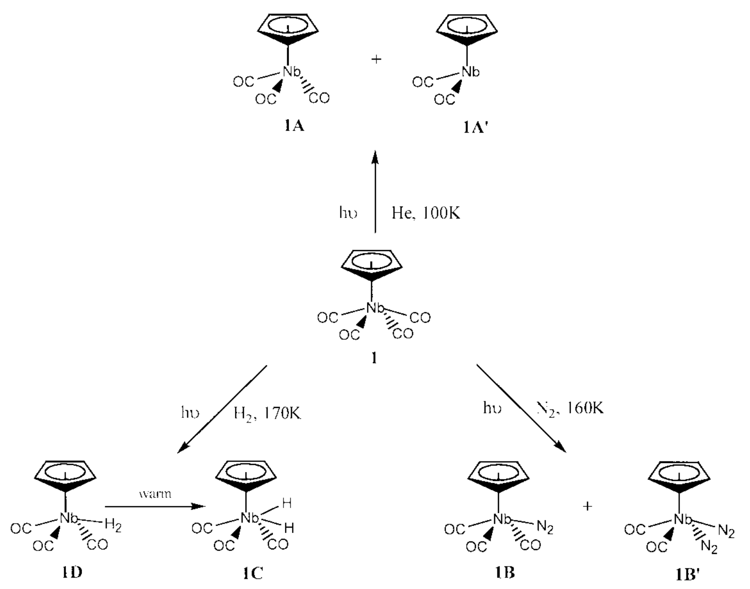

Scheme 1 Diagram showing the reactions of $NbCp(CO)_4$ under He, H_2 and N_2 at low temperature in PE discs.

these complexes in solution at room temperature using TRIR spectroscopy.

Conclusion

This paper has described the spectroscopic characterisation of a number of unstable organometallic dihydrogen, dihydride and dinitrogen compounds in polyethylene (PE) discs (see Schemes 1–4). The use of polymer discs as the matrix material has reproduced and extended the results of the previous liquid xenon experiments. We have shown that the compounds $M(C_9H_7)(CO)_4$ (M = Nb (**3**) or Ta (**4**)) undergo similar reactions to their cyclopentadienyl analogues (**1** and **2**), with the exception of the reactions under hydrogen where **1** forms both a classical dihydride (**1C**) and a non-classical dihydrogen complex (**1D**) whereas **3** forms only the non-classical complex (**3D**). The Ta complexes (**2** and **4**) both form classical dihydrides (**2C** and **4C**). We have performed gas exchange reactions, showing that the dinitrogen complexes **2B** and **4B** react thermally with hydrogen to produce the dihydrides **2C** and **4C**. Preliminary room temperature experiments have shown that the indenyl complex, **4C**, is far more reactive (*ca.* 50 times) than the corresponding Cp complex (**2C**). Unfortunately the other hydrogen and nitrogen bound complexes characterised in this study are too short-lived to have their kinetics measured using conventional FTIR. We are investigating the reactivities of these hydrogen and nitrogen bound complexes at room temperature in *n*-heptane using TRIR, and these results will be the subject of a further publication.

Experimental

The apparatus used for low temperature polymer matrix isolation studies has been described in detail elsewhere.[31,39] Briefly, a 250 μm polyethylene (PE) disc (Hostalen GUR-415 PE (Hoechst)) is impregnated with the organometallic compound under investigation. Impregnation is facile and achieved by placing a PE disc in a solution of organometallic compound dissolved in organic solvent. Once impregnated the disc is fixed inside a high pressure–low temperature (HPLT) copper cell. The cell is filled with reactant gas (typically He, H_2 or N_2) and cooled to the required temperature using an Air Products

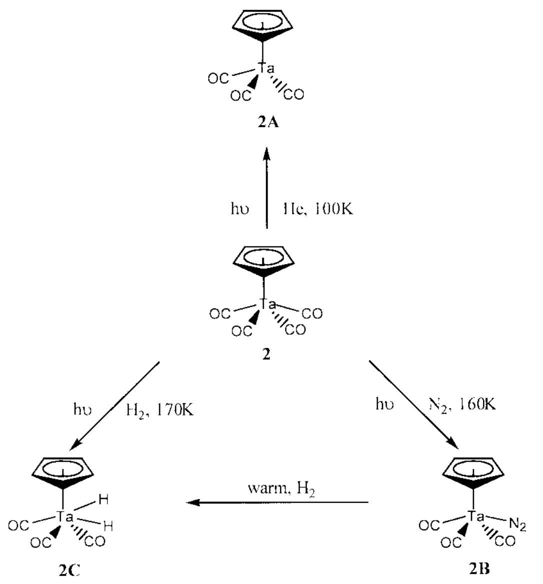

Scheme 2 Diagram showing the reactions of $TaCp(CO)_4$ under He, H_2 and N_2 at low temperature in PE discs.

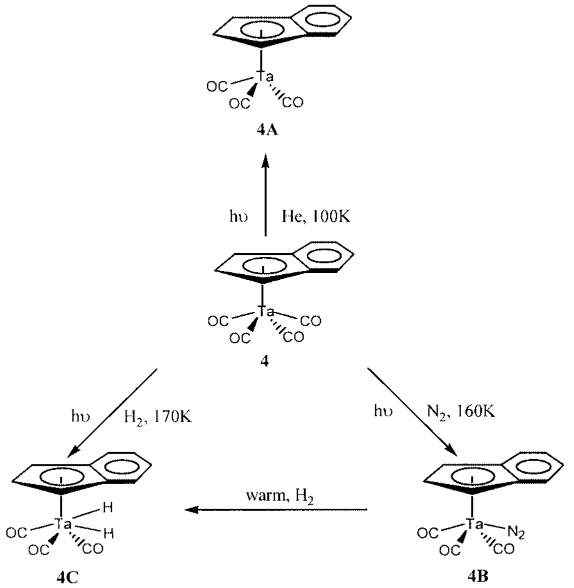

Scheme 4 Diagram showing the reactions of $Ta(C_9H_7)(CO)_4$ under He, H_2 and N_2 at low temperature in PE discs.

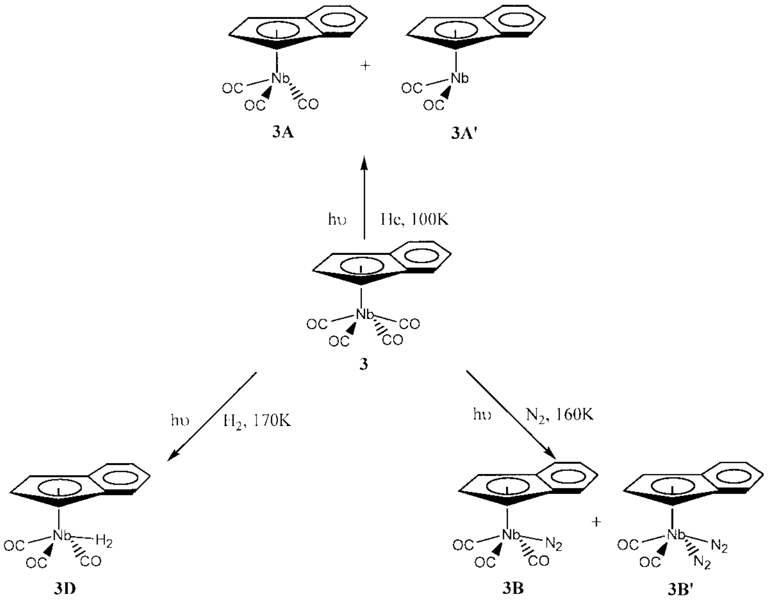

Scheme 3 Diagram showing the reactions of $Nb(C_9H_7)(CO)_4$ under He, H_2 and N_2 at low temperature in PE discs.

Displex CS-202 cooler. Temperatures are accurately measured using a Scientific Instruments Inc. 9600-1 silicon diode temperature controller. Reactions are initiated using broadband UV from a Phillips HPK 125 W medium-pressure mercury arc. and monitored using a Nicolet 730 FTIR Interferometer linked to a PC running OMNIC software. Polyethylene has very weak temperature dependent IR absorptions in the ν(CO) region, therefore background spectra were recorded with PE discs over the range of temperatures required for the experiments, before impregnation of the samples.

The liquid xenon experiments were carried out using the same apparatus. The organometallic compound was placed in the HPLT cell which was then filled with xenon. The cell was cooled to low temperature and photochemical reactions initiated and monitored.

$NbCp(CO)_4$ **1**, $TaCp(CO)_4$ **2**, $Nb(C_9H_7)(CO)_4$ **3** and $Ta(C_9H_7)(CO)_4$ **4** were prepared using a literature procedure.[26] *n*-Pentane, distilled over CaH_2, was used for solvent impregnation of the PE discs. Helium (Air Products, Premier Grade), hydrogen (BOC, Research Grade), nitrogen (Air Products, Premier Grade), xenon (BOC, Research Grade) and carbon monoxide (Air Products, Premier Grade) were used as supplied without further purification.

Acknowledgements

We are grateful to the University of Nottingham for funding and to Dr D. C. Grills, Professor M. Poliakoff and Professor J. J. Turner for their helpful discussions. We thank Mr M. Guyler and K. Stanley for their technical support.

References and notes

1 R. H. Crabtree, *Chem. Rev.*, 1985, **85**, 245.
2 D. M. Heinekey and W. J. Oldham, *Chem. Rev.*, 1993, **93**, 913.
3 M. A. Esteruelas and L. A. Oro, *Chem. Rev.*, 1998, **98**, 577.
4 G. J. Kubas, R. R. Ryan, B. I. Swanson, P. J. Vergamini and H. J. Wasserman, *J. Am. Chem. Soc.*, 1984, **106**, 451.
5 R. R. Eady and G. J. Leigh, *J. Chem. Soc., Dalton Trans.*, 1994, 2739.
6 M. Hidai and Y. Mizobe, *Chem. Rev.*, 1995, **95**, 1115.
7 D. W. Ball, L. Fredin, Z. H. Kafafi, R. H. Hague and J. L. Margrave, *A Bibliography of Matrix Isolation Spectroscopy: 1952–1997*, Rice University Press, Houston, TX, 1988.
8 D. W. Ochsner, D. W. Ball and Z. H. Kafafi, *A Bibliography of Matrix Isolation Spectroscopy: 1985–1997*, NRL Publication NRL/PU/5610/98/357, Naval Research Laboratory, Washington, DC, 1998.
9 J. K. Burdett, A. J. Downs, G. P. Gaskill, M. A. Graham, J. J. Turner and R. F. Turner, *Inorg. Chem.*, 1978, **17**, 523.
10 R. L. Sweany, *J. Am. Chem. Soc.*, 1985, **107**, 2374.
11 R. L. Sweany, *J. Am. Chem. Soc.*, 1986, **108**, 6986.
12 R. L. Sweany, *Organometallics*, 1986, **5**, 387.
13 G. A. Ozin and J. Garciaprieto, *J. Am. Chem. Soc.*, 1986, **108**, 3099.
14 R. K. Upmacis, G. E. Gadd, M. Poliakoff, M. B. Simpson, J. J. Turner, R. Whyman and A. F. Simpson, *J. Chem. Soc., Chem. Commun.*, 1985, 27.
15 R. K. Upmacis, M. Poliakoff and J. J. Turner, *J. Am. Chem. Soc.*, 1986, **108**, 3645.
16 G. E. Gadd, R. K. Upmacis, M. Poliakoff and J. J. Turner, *J. Am. Chem. Soc.*, 1986, **108**, 2547.
17 S. A. Jackson, R. K. Upmacis, M. Poliakoff, J. J. Turner, J. K. Burdett and F. W. Grevels, *J. Chem. Soc., Chem. Commun.*, 1987, 678.
18 S. M. Howdle and M. Poliakoff, *J. Chem. Soc., Chem. Commun.*, 1989, 1099.
19 S. M. Howdle, M. A. Healy and M. Poliakoff, *J. Am. Chem. Soc.*, 1990, **112**, 4804.
20 J. A. Banister, P. D. Lee and M. Poliakoff, *Organometallics*, 1995, **14**, 3876.
21 S. P. Church, F. W. Grevels, H. Hermann and K. Schaffner, *J. Chem. Soc., Chem. Commun.*, 1985, 30.
22 S. A. Jackson, P. M. Hodges, M. Poliakoff, J. J. Turner and F. W. Grevels, *J. Am. Chem. Soc.*, 1990, **112**, 1221.
23 P. M. Hodges, S. A. Jackson, J. Jacke, M. Poliakoff, J. J. Turner and F. W. Grevels, *J. Am. Chem. Soc.*, 1990, **112**, 1234.
24 R. B. Hitam and A. J. Rest, *Organometallics*, 1989, **8**, 1598.
25 A. J. Rest, M. Herberhold and M. Schrepfermann, *Organometallics*, 1992, **11**, 3646.
26 T. E. Bitterwolf, S. Gallagher, J. T. Bays, B. Scallorn, A. L. Rheingold, I. A. Guzei, L. LiableSands and J. C. Linehan, *J. Organomet. Chem.*, 1998, **557**, 77.
27 P. T. Snee, H. Yang, K. T. Kotz, C. K. Payne and C. B. Harris, *J. Phys. Chem. A*, 1999, **103**, 10426.
28 M. T. Haward, M. W. George, S. M. Howdle and M. Poliakoff, *J. Chem. Soc., Chem. Commun.*, 1990, 913.
29 M. T. Haward, M. W. George, P. Hamley and M. Poliakoff, *J. Chem. Soc., Chem. Commun.*, 1991, 1101.
30 M. W. George, M. T. Haward, P. A. Hamley, C. Hughes, F. P. A. Johnson, V. K. Popov and M. Poliakoff, *J. Am. Chem. Soc.*, 1993, **115**, 2286.
31 A. I. Cooper and M. Poliakoff, *Chem. Phys. Lett.*, 1993, **212**, 611.
32 R. H. Hooker and A. J. Rest, *J. Chem. Phys.*, 1985, **82**, 3871.
33 S. E. J. Goff, T. F. Nolan, M. W. George and M. Poliakoff, *Organometallics*, 1998, **17**, 2730.
34 The relative intensities of the symmetric and antisymmetric ν(C–O) vibrations, I_{sym} and I_{asym}, are related by the expression $I_{asym}/I_{sym} = \tan^2(\theta/2)$, where θ is the angle between the two CO groups. Using this relationship it is possible to estimate that the angle between the two CO groups in **1A′** and **3A′** is *ca.* 70°, suggesting that the observed bands are due to the *cis* isomer. This angle also indicates that the dicarbonyl-loss species (**1A′** and **3A′**) have a pyramidal geometry, suggesting that the polymer matrix fills the vacant site on the compound, acting as a “token ligand”. A similar approach can be used to determine that the bis-dinitrogen species **1B′** and **3B′** are of the *cis* geometry.
35 Additional bands at 2020, 1980 and 1905 cm^{-1} are observed following prolonged irradiation of compound **4** under H_2. These are not observed in the absence of H_2 and therefore are likely to be due to a hydrogen bound species, possibly a ring-slipped complex. Similarly additional bands at 2020, 1983 and 1956 cm^{-1} are seen following prolonged irradiation of **2**, which again may be due to a ring-slipped species.
36 R. H. Crabtree and D. G. Hamilton, *J. Am. Chem. Soc.*, 1986, **108**, 3124.
37 M. E. Rerek, L. N. Ji and F. Basolo, *J. Chem. Soc., Chem. Commun.*, 1983, 1208.
38 K. L. McFarlane, B. Lee, W. F. Fu, R. van Eldik and P. C. Ford, *Organometallics*, 1998, **17**, 1826.
39 A. I. Cooper, PhD Thesis, University of Nottingham, 1994.